

**METHODS ARTICLE**

---

# Ammonium–Chloride–Potassium Lysing Buffer Treatment of Fully Differentiated Cells Increases Cell Purity and Resulting Neotissue Functional Properties

Wendy E. Brown, BS,<sup>1</sup> Jerry C. Hu, PhD,<sup>1</sup> and Kyriacos A. Athanasiou, PhD, PE<sup>1,2,\*</sup>

Juvenile and fetal, primary, fully differentiated cells are widely considered to be ideal cell types for tissue engineering applications. However, their use in tissue engineering may be hindered through contamination by undesirable cell types. These include blood-associated cells as well as unwanted resident cell types found both in healthy and pathologic donor tissues. Ammonium–chloride–potassium (ACK) lysing buffer is used to lyse red blood cells (RBCs) during the isolation of stem cell populations, but has not been explored for the purification of fully differentiated cells. This study sought to investigate the effect of ACK buffer treatment of freshly isolated, fully differentiated cells to increase cell purity and enhance the formation of biofunctional engineered neotissues; this was tested in the well-established cartilage tissue engineering model of the self-assembling process using fetal ovine articular chondrocytes (foACs) and juvenile bovine articular chondrocytes (jbACs). ACK buffer treatment of foACs and jbACs decreased the number of contaminating RBCs by over 60% and additionally reduced the number of apoptotic chondrocytes in the cell isolates. Reducing the number of contaminating RBCs removed cellular detractors to the self-assembling process and eliminated an apoptotic stimulus, thus improving neo-cartilage homogeneity, chondrocyte distribution, and extracellular matrix deposition within the neotissues. For example, in foAC neocartilage, ACK buffer treatment ultimately led to a 170% increase in compressive aggregate modulus, a 130% increase in shear modulus, an 80% increase in tensile modulus, and a 130% increase in ultimate tensile strength of the neocartilage. This work represents the first time that ACK buffer has been used to purify fully differentiated cells and subsequently increase the functional properties of neotissue.

## Introduction

**T**HE GOAL OF tissue engineering is to replace injured tissue in an effort to halt and reverse disease progression. Primary, fully differentiated cells are widely considered to be the ideal cell type for tissue engineering. They are phenotypically stable and readily produce tissue-specific extracellular matrix (ECM) molecules. Juvenile, and furthermore fetal, sources of tissue are most desirable due to their enhanced proliferative and synthetic abilities compared with adult cells.<sup>1</sup> Tissue-engineered products comprising juvenile cells are currently used clinically. For example, RevaFlex (ISTO Technologies),<sup>2</sup> a tissue-engineered product for the repair of cartilage using juvenile chondrocytes, is currently in Phase III clinical trials in the United States.<sup>3</sup> While these engineered tissues show promise, they have yet to recapitulate native tissue properties and structure.

Tissue engineering efforts using primary cells may be hindered through contamination by undesirable cell types.

Predominantly, contamination by blood and surrounding tissue can occur during the isolation of target donor tissue. Furthermore, many tissues comprise multiple cell types, not all of which are suitable for tissue engineering applications. Disease state and tissue maturity may additionally introduce unwanted cell phenotypes into isolated populations. Aged tissues, which are more prone to diseases such as cancer, atherosclerosis, and osteoarthritis, contain senescent cells that increasingly produce reactive oxygen species, inflammatory mediators, and matrix-degrading enzymes.<sup>4,5</sup> Regardless of the donor tissue type and age, contamination by hematopoietic cells through blood remains the primary, ubiquitous source of unwanted cell types in cell isolates.<sup>6–9</sup> These limitations necessitate the use of cell purification methods during isolation to eliminate the presence of undesirable phenotypes and achieve homogeneous cell populations suitable for tissue engineering.

Articular cartilage tissue engineering is well established and therefore may be used as an example system. Unwanted cell

---

Departments of <sup>1</sup>Biomedical Engineering and <sup>2</sup>Orthopaedic Surgery, University of California, Davis, California.

phenotypes in cartilage cell isolates can be present due to a number of reasons. The most prevalent is through contamination by hematopoietic cells when taking cartilage biopsies in clinical applications, such as autologous chondrocyte implantation.<sup>7</sup> Crucially, it has been shown that even short-term exposure of cartilage to blood induces chondrocyte apoptosis.<sup>10–12</sup> Second, in a clinical setting, autologous or allogeneic cartilage grafts are often taken from adult tissues, which exhibit matrix degradation, surface defects, and fibrillation.<sup>13</sup> Diseased cartilage, such as in osteoarthritis, experiences enhanced ECM degeneration and contains chondrocytes of altered phenotypes.<sup>13,15–17</sup> Degenerative changes to the cartilage ECM are associated with chondrocyte apoptosis.<sup>14</sup> Fetal cartilage, on the other hand, is vascularized, thus introducing blood and a plethora of cell types into the mass of tissue from which chondrocytes are isolated.<sup>18</sup> Additionally, even in healthy tissue, cartilage isolation itself causes tissue damage, resulting in necrosis at the wound edge and a wave of apoptosis extending into the tissue.<sup>19,20</sup> Cell phenotype heterogeneity, especially by red blood cell (RBC) contamination, may be an unexpected factor limiting the ability of engineered cartilage properties from reaching those of native tissue.

Despite the need for chondrocyte purification, only a few studies have aimed to demonstrate its importance. Employing collagenase to sequentially digest whole hamster rib cartilage into two fractions, it was demonstrated that the second fraction contained a cell population with more homogeneous chondrocytic morphology compared with the whole unseparated population.<sup>21</sup> Another method to purify isolated chondrocytes is through sequential plating. Rat cartilage cell isolates separated by differential adhesion to tissue culture plastic showed 100% chondrocytes after the 8<sup>th</sup> plating versus a mixture of cells when the whole population was plated.<sup>22</sup> Yet another method suggests the use of cell surface markers, such as CD14 and CD45, to exclude contamination by monocytes and hematopoietic cells.<sup>7</sup> Ammonium–chloride–potassium (ACK) lysing buffer is commonly used to lyse RBCs in samples containing white blood cells, such as ethylenediaminetetraacetic acid (EDTA)-treated whole blood, buffy coats, and bone marrow. For tissue engineering purposes, ACK buffer is used to isolate pure populations of stem cells, such as adipose-derived<sup>23,24</sup> and mesenchymal stem cells,<sup>25</sup> but has not yet been explored in the isolation of non-stem cell types. As RBCs are the primary, ubiquitous contaminating cell type in many isolates of fully differentiated cells, including chondrocytes, ACK buffer treatment holds promise for purification of the cell populations desirable for tissue engineering applications.

Given the importance of cell purity, the objective of this study was to determine the utility of ACK buffer treatment of freshly isolated fully differentiated cells to enhance their capacity to form bifunctional tissues. Clinically relevant articular chondrocytes (ACs) from fetal and juvenile cartilage were used as the model in the following studies: in Study 1, fetal ovine articular chondrocytes (foACs) were treated with ACK buffer during their isolation. It was hypothesized that treatment would increase chondrocyte purity and subsequently increase the functional properties of self-assembling neocartilage. In Study 2, it was the goal to confirm the effects of ACK buffer treatment on cells from an animal model of different species and age, specifically juvenile bovine articular chondrocytes (jbACs).

## Materials and Methods

### Cell isolation

foACs were harvested from the patellofemoral surfaces of the stifle joints of three fetal (120–125 day gestation), female, Dorper cross sheep (UC Davis Veterinary Medical School, Davis, CA). jbACs were harvested from the patellofemoral surfaces of the stifle joints of three juvenile (2–14 days), male, Holstein and Jersey calves (Research 87). Processing of ovine and bovine tissues was the same. Articular cartilage from the whole surface of both condyles and the trochlear groove was minced into ~1 mm<sup>3</sup> pieces, then washed and centrifuged (500 g for 5 min) three times with Dulbecco's modified Eagle's medium containing 4.5 g/L glucose and GlutaMAX (DMEM; Gibco) and 2% (v/v) penicillin/streptomycin/fungizone (PSF; BD Biosciences). The tissue was digested in 0.2% (w/v) collagenase type II (Worthington) in DMEM containing 3% (v/v) fetal bovine serum (Atlanta Biologicals) for 18 h at 37°C with gentle rocking. After digestion, the resultant cell solutions were filtered through 70- $\mu$ m cell strainers, centrifuged (500 g for 5 min), and resuspended in blank DMEM. ACs and RBCs were counted and the viability of ACs was assessed by Trypan Blue staining. Half of the foACs and half of the jbACs were treated with ACK buffer, as described in detail below. Cells were counted and viability was assessed again after ACK buffer treatment. Untreated cells were washed with blank DMEM instead of ACK buffer, but were otherwise handled the same way. Cells immediately underwent self-assembly.

### ACK buffer treatment

The ACK buffer consisted of 154.4 mM ammonium chloride (Sigma), 10 mM potassium bicarbonate (Sigma-Aldrich), and 97.3  $\mu$ M EDTA tetrasodium salt (Acros Organics). This corresponds to 8.26 g ammonium chloride, 1.0 g potassium bicarbonate, and 0.037 g EDTA in 1 L of ultrapure water. This solution should be sterile filtered before use. The protocol for using ACK buffer to purify chondrocytes consists of the following steps:

1. Warm ACK buffer to 37°C.
2. Portion up to 100 million chondrocytes into a 50-mL conical tube.
3. Centrifuge the cell solution at 500 g for 5 min.
4. Aspirate the supernatant and gently resuspend the cell pellet in 10 mL of ACK buffer. Incubate for 3–5 min at 37°C.
5. Centrifuge the ACK buffer cell suspension at 500 g for 5 min.
6. Aspirate the ACK buffer. Wash the cell pellet twice with blank or washing medium before plating or freezing.

### Neocartilage construct seeding and culture

Primary foACs and jbACs treated with ACK buffer (+ACK Treatment) and untreated (–ACK Treatment) were each self-assembled into engineered neocartilage constructs in nonadherent agarose wells. A sterile stainless steel mold consisting of 5 mm diameter cylindrical posts was inserted into a 48-well plate, each well containing 1 mL molten 2% (w/v) molecular biology-grade agarose (Thermo) to create a single agarose well in each plate well. After solidification of the agarose at room temperature, the mold was removed.

Agarose wells were filled with chemically defined chondrogenic medium (CHG medium) (DMEM containing 1% PSF, 1% ITS+premix (BD Biosciences), 1% nonessential amino acids (Gibco), 100 nM dexamethasone (Sigma), 50 mg/mL ascorbate-2-phosphate (Sigma), 40 g/mL L-proline (Sigma), and 100 mg/mL sodium pyruvate (Sigma). CHG medium was exchanged twice over the course of 5 days to ensure saturation of the agarose before cell seeding. Treated and untreated foACs and jbACs were each seeded at 4.5 million cells per construct into 5 mm agarose wells in 100  $\mu$ L CHG medium. Constructs were unconfined at day 6 and placed in larger wells coated with agarose to prevent construct adhesion to the wells. Medium was exchanged daily before unconfinement and every other day after for the duration of the 6-week culture period. Gross morphological analysis, histology, immunohistochemistry (IHC), quantification of glycosaminoglycans (GAGs) and collagen, and mechanical evaluation were performed at the end of the culture period.

**Gross morphological analysis**

Construct thickness was measured from pictures of the constructs using ImageJ software (National Institutes of Health). Whole constructs were weighed to obtain wet weights before samples were portioned for histological, biochemical, and mechanical analysis.

**Histological and immunohistochemical evaluation**

Samples were fixed in 10% neutral buffered formalin, embedded in paraffin, and sectioned along the short axis into 5  $\mu$ m sections to expose the full thickness of the construct. Sections were stained with Hematoxylin and Eosin to show morphology, Safranin O/Fast Green to visualize GAGs, and Picrosirius Red to visualize collagen. Additionally, IHC was performed for collagen I (ab90395, dilution 1:250; Abcam) and collagen II (ab34712, dilution 1:4000; Abcam).

**Biochemical evaluation**

Before construct seeding, caspase activity in ACK-treated and untreated cells was determined with a Caspase-Glo 3/7 assay (Promega). Caspase activity was normalized to DNA content, as quantified with PicoGreen dsDNA reagent (Invitrogen). Construct samples portioned for biochemical analysis were weighed to measure wet weights, lyophilized, and weighed again to measure dry weights. Construct hydration was determined by normalizing the difference in weights before and after lyophilization to the sample wet weight. Lyophilized samples were digested in 125  $\mu$ g/mL papain (Sigma-Aldrich) at 65°C for 18 h. GAG content was quantified by a Blyscan assay kit (Biocolor). Collagen content was quantified by a modified colorimetric chloramine-T hydroxyproline assay.<sup>26</sup> A standard curve was generated using a Sircol collagen standard (Biocolor). DNA content was quantified with PicoGreen dsDNA reagent (Invitrogen). Both collagen and GAG contents were normalized to wet weight, dry weight, and DNA content.

**Mechanical evaluation**

Creep indentation compressive testing was performed on 3 mm diameter punches from each construct. A 0.8 mm diameter, flat, porous indenter tip was applied to the samples using masses ranging from 0.45 to 2 g to achieve 10–15%

strain. A semianalytical, seminumerical, linear biphasic model and a finite element model were used to obtain the aggregate and shear moduli from the experimental data.<sup>27</sup> For tensile testing, samples were punched into dog bone-shaped specimens with gauge lengths of 1.92 mm, adherent to ASTM standards (ASTM D3039). Paper tabs were glued to the samples outside the gauge length, gripped in a TestResources machine (TestResources, Inc.), and pulled at 1% of the gauge length per second until sample failure. The cross-sectional area of samples was measured with ImageJ and used to generate a stress–strain curve. The tensile modulus was obtained by a least-squares fit of the linear region of the curve. The maximum stress yielded the ultimate tensile strength (UTS).

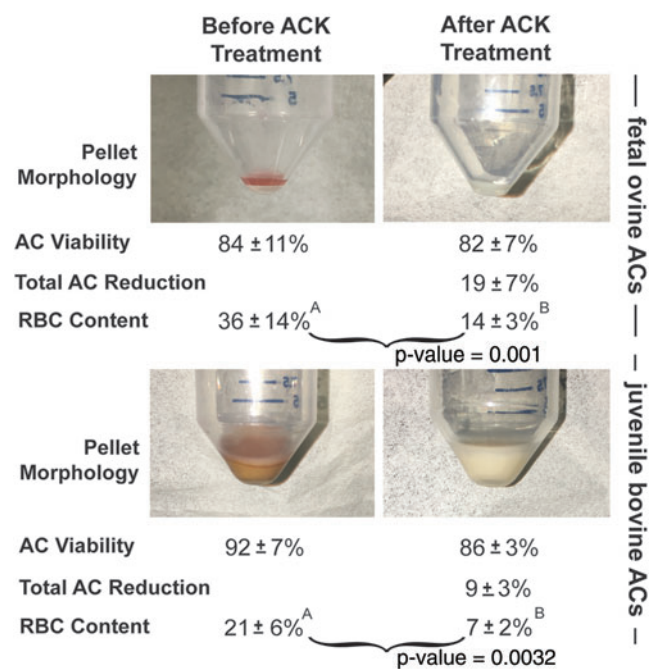
**Statistical analysis**

Student’s *t*-test in Prism 6 (GraphPad Software) was used to analyze the biochemical and mechanical data. A *p* value of <0.05 indicated statistical significance. A sample size of *n*=6 per group was used. In figures displaying quantitative results, groups marked by different letters are statistically different. All data are presented as means  $\pm$  standard deviations.

**Results**

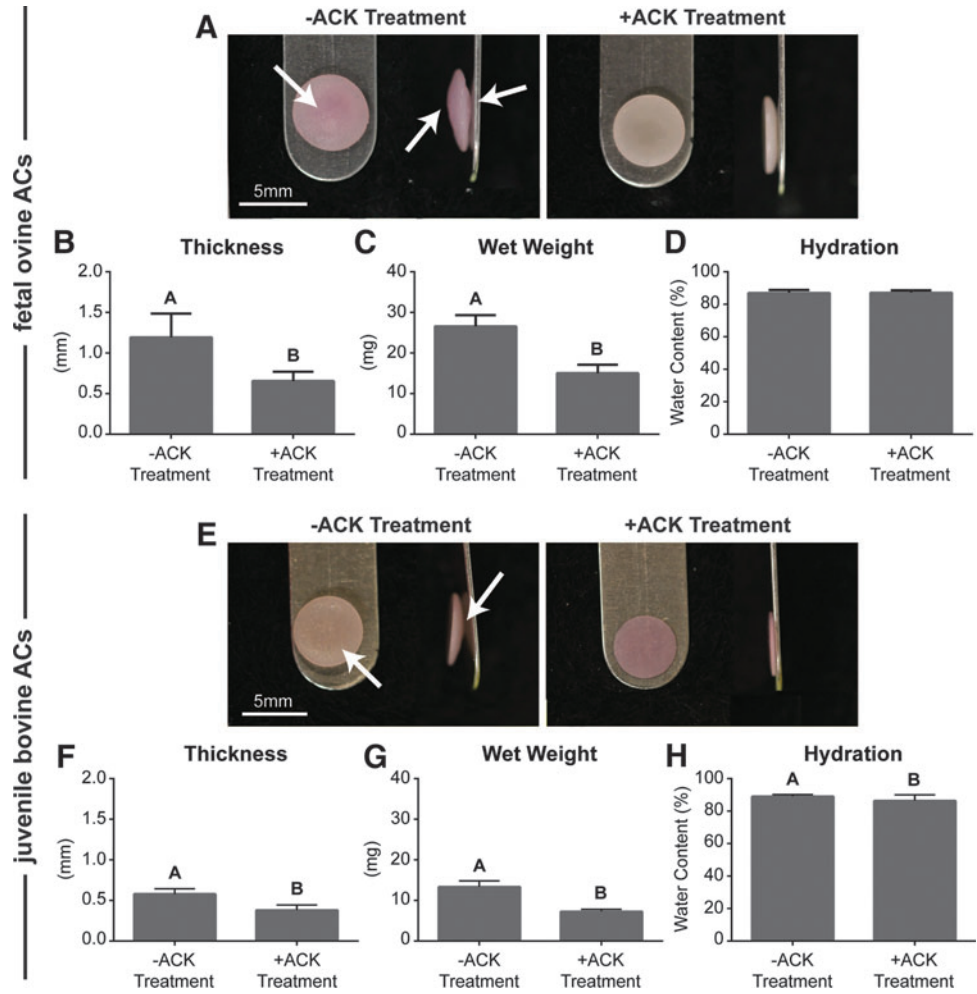
**Chondrocyte viability and purity**

Figure 1 illustrates the isolated cell pellet morphology and cell counts before and immediately after ACK buffer treatment. ACK buffer treatment resulted in a morphological



**FIG. 1.** Immediate effect of ACK treatment. ACK treatment of freshly isolated foACs and jbACs resulted in a change in cell pellet color and a significant reduction in RBC content. AC, articular chondrocyte; ACK, ammonium–chloride–potassium; foAC, fetal ovine articular chondrocyte; jbAC, juvenile bovine articular chondrocyte; RBC, red blood cell. Statistical significance is denoted by marking groups with different letters. Statistical significance is indicated with a *p*-value <0.05. (See the Statistical analysis section.) Color images available online at [www.liebertpub.com/tec](http://www.liebertpub.com/tec)

**FIG. 2.** Neocartilage gross morphology. Untreated foAC and jbAC neocartilages (A and E, respectively) contained bulbous diffuse regions that were eliminated with ACK treatment. Treatment also reduced fetal ovine and juvenile bovine neocartilage thicknesses (B, F) and wet weights (C, G). ACK treatment reduced jbAC neocartilage hydration (H), but not foAC neocartilage hydration (D). Color images available online at [www.liebertpub.com/tec](http://www.liebertpub.com/tec)



change of the pellets of both cell types. The foAC pellet before treatment appeared light red throughout and milky white after treatment. The jbAC pellet appeared tan with a pink cast before treatment and milky white after treatment. Viability of foACs before and after treatment was  $84\% \pm 11\%$

and  $82\% \pm 7\%$ , respectively. Viability of jbACs before treatment was  $92\% \pm 7\%$  and after treatment was  $86\% \pm 3\%$ . The total number of foACs and jbACs was reduced by  $19\% \pm 7\%$  and  $9\% \pm 3\%$ , respectively, with ACK treatment. RBC content was significantly reduced after treatment of both

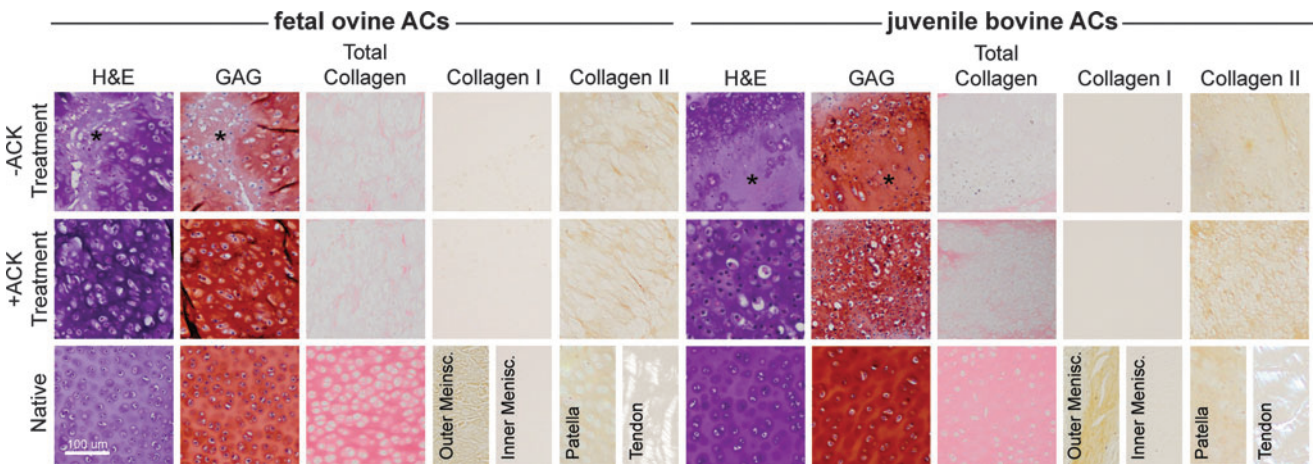


**FIG. 3.** Neocartilage histology. ACK treatment of foACs and jbACs eliminated the diffuse regions of low cellularity present in untreated constructs (\*), enhanced neocartilage homogeneity, and intensified GAG, total collagen, and collagen II staining. GAG, glycosaminoglycan. Color images available online at [www.liebertpub.com/tec](http://www.liebertpub.com/tec)

foACs ( $36\% \pm 14\%$  before and  $14\% \pm 3\%$  after treatment) and jbACs ( $21\% \pm 6\%$  before and  $7\% \pm 2\%$  after).

#### Self-assembled neocartilage morphology

Figure 2 shows the gross morphology of self-assembled neocartilage constructs after 6 weeks of culture. All constructs appeared hyaline-like with similar diameters. Bulbous diffuse regions were present within both foAC and jbAC untreated groups. ACK treatment eliminated these regions and yielded flat foAC and jbAC neocartilage. ACK treatment also reduced the thickness and wet weight of both foAC and jbAC neocartilage constructs. Thickness of foAC neocartilage was  $1.2 \pm 0.1$  mm without treatment and was significantly reduced to  $0.7 \pm 0.1$  mm with treatment. Thickness of jbAC neocartilage was  $0.58 \pm 0.1$  mm without treatment and was significantly reduced to  $0.38 \pm 0.1$  mm with treatment. Wet weight of foAC neocartilage was  $26.6 \pm 0.8$  mg without treatment and was significantly reduced to  $15.1 \pm 0.6$  mg with treatment. Wet weight of jbAC neocartilage without treatment was  $13.3 \pm 0.4$  mg and was significantly reduced to  $7.3 \pm 0.2$  mg with treatment. Hydration of foAC neocartilage was  $87.1\% \pm 0.5\%$  without ACK treatment and  $87.2\% \pm 0.4\%$  with treatment. Hydration of jbAC neocartilage was  $89.0\% \pm 0.3\%$  without ACK treatment and was significantly reduced to  $86.4\% \pm 0.9\%$  with treatment.

#### Histological and immunohistochemical assessment

Figure 3 shows neocartilage construct histology and immunohistochemistry after 6 weeks of culture. Histology showed the presence of diffuse GAG-rich regions of low cellularity in both untreated foAC and jbAC neocartilage. ACK treatment eliminated these diffuse regions, yielding homogeneous tissue staining more intensely for GAG and collagen in both foAC and jbAC constructs. Intense GAG staining was present across all groups, which was further increased with ACK treatment for both foAC and jbAC constructs. Collagen staining was present across all groups, but was additionally enhanced by ACK treatment for both foAC and jbAC constructs. Collagen I staining was not present in either the untreated or treated foAC and jbAC constructs. Collagen II staining was present in both untreated foAC and jbAC constructs and was intensified by ACK treatment.

#### Biochemical content

Figure 4 demonstrates biochemical content of the neocartilage constructs. Cellular caspase activity per DNA in both foACs and jbACs was significantly reduced by ACK treatment. Caspase activity of foACs before ACK treatment was  $31.2 \pm 5.2$  RLU/ng DNA and was significantly reduced to  $12.8 \pm 3.7$  RLU/ng DNA with treatment. Caspase activity of jbACs before ACK treatment was  $56.9 \pm 0.2$  RLU/ng DNA and was significantly reduced to  $40.2 \pm 1.9$  RLU/ng DNA with treatment. Untreated and ACK-treated foAC neocartilage GAG per wet weight (GAG/WW) was  $5.5\% \pm 0.1\%$  and  $5.7\% \pm 0.2\%$ , respectively. Untreated and ACK-treated foAC neocartilage GAG per dry weight (GAG/DW) was  $42.8\% \pm 1.5\%$  and  $43.1\% \pm 1.7\%$ , respectively. GAG per DNA in untreated foAC constructs was  $60.4 \pm 0.9$   $\mu\text{g}/\mu\text{g}$  and was significantly reduced to  $50.54 \pm 1.3$   $\mu\text{g}/\mu\text{g}$  with ACK treatment. ACK treatment significantly decreased jbAC construct GAG per wet weight from  $3.9\% \pm 0.2\%$  to  $3.0\% \pm 0.1\%$  and GAG per dry weight from  $33.5\% \pm 2.0\%$  to

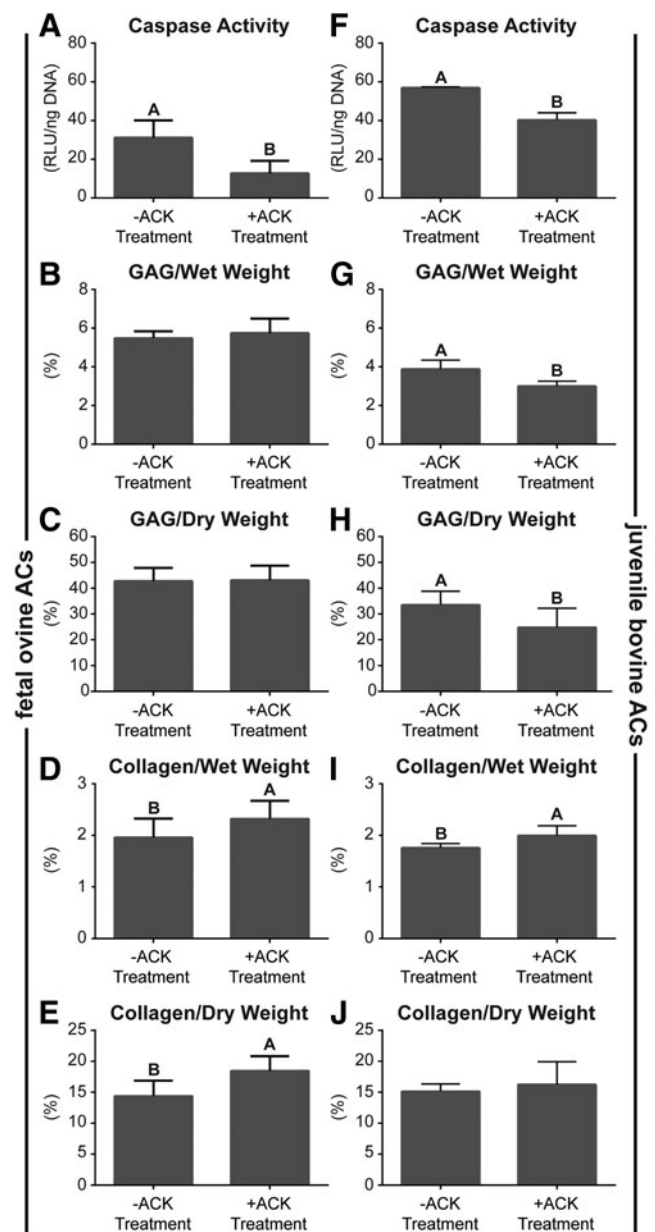


**FIG. 4.** Neocartilage biochemical content. ACK treatment significantly reduced foAC and jbAC caspase activity (A, F), jbAC GAG/WW (G), and jbAC GAG/DW (H). ACK treatment significantly increased foAC and jbAC collagen/WW (D, I) and foAC collagen/DW (E). foAC GAG/WW, GAG/DW, and jbAC collagen/DW (B, C, J) were unaffected.

$24.8\% \pm 2.8\%$ . ACK treatment significantly reduced jbAC construct GAG per DNA from  $70.65 \pm 5.3$  to  $28.1 \pm 1.4$   $\mu\text{g}/\mu\text{g}$ .

Construct collagen per wet weight (collagen/WW) and collagen per dry weight (collagen/DW) in foAC neocartilage were significantly increased from  $2.0\% \pm 0.1\%$  to  $2.3\% \pm 0.1\%$  and  $14.4\% \pm 0.8\%$  to  $18.5\% \pm 0.7\%$ , respectively, by ACK treatment. Construct collagen per DNA in untreated and ACK-treated foAC neocartilage was  $20.5 \pm 0.9$  and  $20.4 \pm 0.8$   $\mu\text{g}/\mu\text{g}$ , respectively. ACK treatment significantly increased collagen per wet weight from  $1.8\% \pm 0.1\%$  to  $2.0\% \pm 0.1\%$  in jbAC constructs. Collagen per dry weight in the untreated jbAC constructs was  $15.2\% \pm 0.5\%$  and  $16.3\% \pm 1.4\%$  in the ACK-

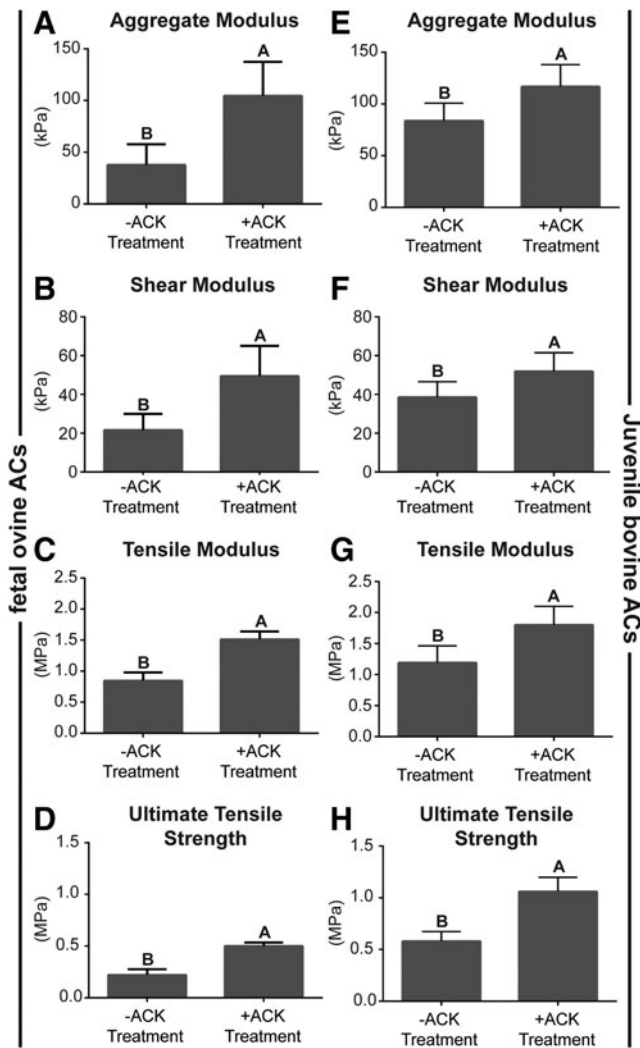


**FIG. 5.** Neocartilage mechanical properties. ACK treatment significantly increased all mechanical (A–H) properties measured for both cell types.

treated constructs. Collagen per DNA in untreated jbAC constructs was  $31.7 \pm 1.2 \mu\text{g}/\mu\text{g}$  and was significantly reduced to  $18.6 \pm 0.7 \mu\text{g}/\mu\text{g}$  with ACK treatment.

#### Mechanical properties

ACK treatment significantly enhanced the compressive, shear, and tensile properties of both foAC and jbAC neocartilage constructs (Fig. 5). Aggregate modulus of foAC constructs significantly increased from  $37.8 \pm 8.1$  to  $104.5 \pm 13.5$  kPa with ACK treatment. ACK treatment similarly and significantly increased jbAC construct aggregate modulus from  $83.8 \pm 7.0$  to  $116.6 \pm 8.8$  kPa. Shear moduli of foAC and jbAC neocartilage were significantly increased from  $21.6 \pm 3.5$  to  $49.4 \pm 6.4$  kPa and  $38.5 \pm 3.3$  to  $51.9 \pm 4.0$  kPa, respectively, by ACK treatment. ACK treatment significantly increased foAC construct tensile modulus from  $0.8 \pm 0.1$  to  $1.5 \pm 0.1$  MPa and UTS from  $0.2 \pm 0.1$  to  $0.5 \pm 0.1$  MPa. Tensile modulus of jbAC constructs significantly increased from  $1.2 \pm 0.1$  to  $1.8 \pm 0.1$  MPa, and UTS significantly increased from  $0.6 \pm 0.1$  to  $1.1 \pm 0.1$  MPa as a result of ACK treatment.

#### Discussion

This study sought to investigate the effect of ACK buffer treatment of freshly isolated, fully differentiated cells to increase cell purity and enhance their ability to form bio-functional engineered neotissues. This was tested in the well-established cartilage tissue engineering model of the self-assembling process. The hypothesis that ACK treatment of ACs from donors of different species and age would each yield neocartilage constructs with improved functional properties compared with constructs formed with untreated cells was confirmed. ACK treatment immediately decreased the number of apoptotic chondrocytes and decreased contamination by unwanted cell types. Treatment also resulted in flat, homogeneous, hyaline-like neocartilage constructs by eliminating the diffuse regions of low cellularity present within the constructs engineered from untreated cells. Finally, treatment yielded neocartilage with superior biochemical composition as well as compressive, shear, and tensile properties. This work represents the first time that ACK buffer has been used to purify fully differentiated cells and demonstrates the significant detrimental effects of contaminating cell types on neotissue functional properties.

Eliminating contaminating cell phenotypes results in improved neocartilage morphology and homogeneity. Treatment resulted in a significant reduction of RBC content in both foAC and jbAC cell isolates (Fig. 1). This yielded increased neocartilage homogeneity by eliminating the diffuse GAG-rich regions of low cellularity observable in histology of the untreated constructs (Fig. 3). These regions are likely responsible for the gross morphological abnormalities observed in the untreated constructs (Fig. 2A, E) and their removal resulted in the reduced tissue thickness observed in treated constructs (Fig. 2B, F). GAG deposition in the diffuse regions is particularly apparent in the jbAC constructs (Fig. 3); the reduction of these regions correlates with the significant decrease in GAG per wet weight, GAG per dry weight, and tissue hydration also seen in the jbAC constructs. The self-assembling process by which the neocartilage constructs in these studies were formed relies on cell–cell contact encouraged by nonadherent surfaces and free energy minimization through differential adhesion and differential tension.<sup>28</sup> The presence of RBCs may have introduced unexpected forces in the culture system as a result of cell sorting and interfered with chondrocyte–chondrocyte communication and subsequent neocartilage formation. Additionally, as blood components, particularly RBCs and mononuclear cells, are known to cause chondrocyte apoptosis,<sup>10,29</sup> eliminating RBCs in culture removed a major cause of chondrocyte death, which may also be responsible for neocartilage inhomogeneity. These results show that removal of cellular detractors to the self-assembling process and eliminating an apoptotic stimulus improves the homogeneity of neocartilage cellular distribution and matrix deposition.

ACK buffer treatment not only eliminated contaminating RBCs but may also have eliminated apoptotic chondrocytes. The total number of chondrocytes was measured before and after ACK treatment using a hemocytometer, and care was taken not to include RBCs, which are much smaller in diameter, into the count. ACK buffer treatment decreased total AC numbers by  $\sim 20\%$  for foACs and  $\sim 10\%$  for jbACs, without significantly reducing AC viability (Fig. 1). The reduction in total AC numbers implies that ACK treatment

potentially removed chondrocytes as well as RBCs. It was then hypothesized that ACK treatment preferentially lysed apoptotic ACs. The activity of executioner caspases 3 and 7, which proteolytically degrade intracellular proteins as part of programmed cell death,<sup>30</sup> was measured. Caspase activity was significantly decreased per ng DNA in both foACs and jbACs after ACK treatment (Fig. 3A, F). The decrease in caspase activity, coupled with the decrease in total AC numbers, implies that ACK buffer reduced the number of apoptotic chondrocytes already present. During apoptosis, caspases break down the cytoskeleton,<sup>31</sup> resulting in membrane blebbing.<sup>32</sup> It is possible that the breakdown of the cytoskeleton within apoptotic chondrocytes renders them unable to withstand the osmotic pressure changes induced by hypotonic ACK buffer application. Additionally, the loss of excess cell membrane through blebbing may not allow for the surface area expansion that takes place in normal chondrocytes under hypotonic conditions.<sup>33</sup> Both cytoskeletal breakdown and loss of cell membrane through blebbing make chondrocytes on the apoptotic pathway more susceptible to ACK buffer-induced cell rupture.<sup>31–33</sup> This suggests that ACK buffer not only lyses RBCs, as expected, but also eliminates apoptotic chondrocytes that are not yet marked dead by traditional viability stains such as Trypan Blue. To our knowledge, this is the first study to document that ACK buffer can be used to purify chondrocyte subpopulations of apoptotic chondrocytes.

Increases in construct mechanical properties can be correlated with biochemical composition and the absence of diffuse regions within the tissue. The aggregate modulus of neocartilage is significantly increased with ACK treatment of both foACs and jbACs (Fig. 5A, D), despite the reduction in GAG content in jbAC constructs (Fig. 4). This implies that GAG content is not the sole contributor to compressive properties and that matrix homogeneity and collagen content may also be key factors. ACK treatment also resulted in more intense collagen staining throughout and significant increases in collagen content across both the foAC and jbAC groups, likely due to increased cellular distribution and subsequent tissue homogeneity. These changes in collagen deposition correspond to significantly increased tensile moduli and UTS in both foAC and jbAC constructs (Fig. 5B, C, E, and F). A material is stronger in the absence of stress concentrations created by ECM discontinuities. It is likely that the improved tissue homogeneity achieved with ACK treatment eliminated stress concentrations caused by abrupt changes in tissue material properties, thus improving the neocartilage mechanical properties in both compression and tension. The importance of a gradual transition between tissues has been shown in composite orthopaedic tissues, such as the cartilage–bone and tendon/ligament–bone interfaces.<sup>34</sup> However, future studies should examine the effects of tissue inhomogeneity on stress concentration development and the subsequent changes in mechanical properties within single orthopaedic tissues. Increased tissue homogeneity achieved by ACK buffer treatment increases neotissue compressive, shear, and tensile moduli.

The impact of blood-induced cartilage death has far-reaching clinical relevance and motivates the identification of exogenous treatments to prevent this damage. This study emphasizes the importance of eliminating blood components in chondrocyte cultures for tissue engineering. Exposure of chondrocytes to blood is not just a concern for

*in vitro* work, however. Clinically used surgical techniques to repair articular cartilage damage, for example, microfracture, drilling, and mosaicplasty, involve the stimulation of bleeding from the subchondral bone plate to access bone marrow-derived mesenchymal stem cells in an effort to stimulate tissue regeneration.<sup>35</sup> Despite the benefits of accessing these cells, short-term exposure of cartilage to blood results in degenerative changes to blood-exposed cartilage.<sup>10</sup> Even rapid clearance of a joint bleed in a canine knee *in vivo* resulted in reduced proteoglycan synthesis rates in exposed cartilage.<sup>11</sup> It also contributed to synovial changes, which caused proteoglycan release from healthy cartilage.<sup>11</sup> The mechanism by which chondrocytes become apoptotic after exposure to blood is unclear. It has been suggested that hydrogen peroxide production by chondrocytes as a result of IL-1 $\beta$  stimulation, in combination with hemoglobin-derived iron, causes an increase in free radical formation, which permanently damages chondrocytes.<sup>10</sup> Therefore, therapeutic approaches to prevent chondrocyte apoptosis may involve targeting IL-1 $\beta$  with antibodies, such as canakinumab,<sup>36</sup> and sequestering iron with compounds such as gallium.<sup>37</sup> In light of the growing body of evidence implicating blood exposure as a stimulus for cartilage damage, further research to elucidate the exact mechanisms involved, its effect on the outcomes of current clinical therapies, and potential therapeutics should be performed.

These studies demonstrated the positive effects of ACK buffer treatment on clinically relevant cell types. Juvenile chondrocytes are more proliferative and more readily produce cartilage-specific matrix than chondrocytes sourced from adult cartilage.<sup>1</sup> As such, juvenile bovine cartilage as a cell source is common for cartilage tissue engineering. As reviewed, many articles have been published using this cell source to investigate the effects of mechanical, biochemical, and bioactive stimuli to form functional neocartilage.<sup>38</sup> Although engineered from animal sources, these tissues pave the way for clinical translation of human juvenile chondrocytes to be used for cartilage therapy. For example, DeNovo NT (Zimmer) is a particulated juvenile cartilage implant used for the allogeneic repair of cartilage damage; its use shows defect filling and clinical improvement in pain and function.<sup>39</sup> RevaFlex (ISTO), formerly DeNovo ET, is a neocartilage engineered from juvenile chondrocytes to repair cartilage defects capable of resurfacing lesions of up to 5 cm<sup>2</sup>.<sup>2</sup> Fetal chondrocytes show an even greater chondrogenic potential than juvenile chondrocytes.<sup>40</sup> This, coupled with the common use of the sheep as an animal model to investigate cartilage repair,<sup>41</sup> makes foACs highly relevant to the clinical translation of fetal chondrocyte tissue-engineered technologies. Given the success of ACK buffer to purify these clinically relevant cell types, this work should be extended into other fully differentiated cell types for tissue engineering.

## Conclusions

This study underscores the importance of cell purity to the success of tissue engineering efforts. ACK buffer treatment of foACs and jbACs produced homogeneous, hyaline-like neocartilage constructs. Treatment reduced the number of contaminating RBCs by over 60% and reduced caspase activity in both cell isolates. Furthermore, tissue homogeneity and distribution of chondrocytes and cartilage-specific matrix

components were greatly increased. Increased ECM homogeneity subsequently increased tissue compressive aggregate modulus by 170%, increased shear modulus by 130%, increased tensile modulus by 80%, and increased UTS by 130%. To the authors' knowledge, this is the first time that ACK buffer has been used to purify freshly isolated fully differentiated cells. The lack of existing chondrocyte purification methods and the improved functional properties achieved with ACK treatment suggest that the presence of contaminating cell types within cartilage cultures may be a significant limiting factor to achieving native tissue properties in not only engineered neocartilage but also other neotissues from fully differentiated cells.

### Acknowledgment

This work was supported by the National Institutes of Health R01 AR067821.

### Disclosure Statement

No competing financial interests exist.

### References

- Adkisson, H.D.t., Martin, J.A., Amendola, R.L., Milliman, C., Mauch, K.A., Katwal, A.B., Seyedin, M., Amendola, A., Streeter, P.R., and Buckwalter, J.A. The potential of human allogeneic juvenile chondrocytes for restoration of articular cartilage. *Am J Sports Med* **38**, 1324, 2010.
- McCormick, F., Cole, B.J., Nwachukwu, B., Harris, J.D., Adkisson, H.D.I.V., and Farr, J. Treatment of focal cartilage defects with a juvenile allogeneic 3-dimensional articular cartilage graft. *Operat Tech Sports Med* **21**, 95.
- Neocartilage Implant to Treat Cartilage Lesions of the Knee. <https://www.clinicaltrials.gov/ct2/show/NCT01400607?term=RevaFlex&rank=1> (accessed February 29, 2016).
- Freund, A., Orjalo, A.V., Desprez, P.Y., and Campisi, J. Inflammatory networks during cellular senescence: causes and consequences. *Trends Mol Med* **16**, 238, 2010.
- Naik, E., and Dixit, V.M. Mitochondrial reactive oxygen species drive proinflammatory cytokine production. *J Exp Med* **208**, 417, 2011.
- Assmus, B., Tonn, T., Seeger, F.H., Yoon, C.H., Leistner, D., Klotsche, J., Schachinger, V., Seifried, E., Zeiher, A.M., and Dimmeler, S. Red blood cell contamination of the final cell product impairs the efficacy of autologous bone marrow mononuclear cell therapy. *J Am Coll Cardiol* **55**, 1385, 2010.
- Kruger, M., Kruger, J.P., Kinne, R.W., Kaps, C., and Endres, M. Are surface antigens suited to verify the redifferentiation potential and culture purity of human chondrocytes in cell-based implants. *Tissue Cell* **47**, 489, 2015.
- Caterson, E.J., Nesti, L.J., Danielson, K.G., and Tuan, R.S. Human marrow-derived mesenchymal progenitor cells: isolation, culture expansion, and analysis of differentiation. *Mol Biotechnol* **20**, 245, 2002.
- Kisiday, J.D., Goodrich, L.R., McIlwraith, C.W., and Frisbie, D.D. Effects of equine bone marrow aspirate volume on isolation, proliferation, and differentiation potential of mesenchymal stem cells. *Am J Vet Res* **74**, 801, 2013.
- Hooiveld, M., Roosendaal, G., Wenting, M., van den Berg, M., Bijlsma, J., and Lafeber, F. Short-term exposure of cartilage to blood results in chondrocyte apoptosis. *Am J Pathol* **162**, 943, 2003.
- Jansen, N.W., Roosendaal, G., Wenting, M.J., Bijlsma, J.W., Theobald, M., Hazewinkel, H.A., and Lafeber, F.P. Very rapid clearance after a joint bleed in the canine knee cannot prevent adverse effects on cartilage and synovial tissue. *Osteoarthritis Cartilage* **17**, 433, 2009.
- Madhok, R., Bennett, D., Sturrock, R.D., and Forbes, C.D. Mechanisms of joint damage in an experimental model of hemophilic arthritis. *Arthritis Rheum* **31**, 1148, 1988.
- Hollander, A.P., Pidoux, I., Reiner, A., Rorabeck, C., Bourne, R., and Poole, A.R. Damage to type II collagen in aging and osteoarthritis starts at the articular surface, originates around chondrocytes, and extends into the cartilage with progressive degeneration. *J Clin Invest* **96**, 2859, 1995.
- Thomas, C.M., Fuller, C.J., Whittles, C.E., and Sharif, M. Chondrocyte death by apoptosis is associated with cartilage matrix degradation. *Osteoarthritis Cartilage* **15**, 27, 2007.
- Yagi, R., McBurney, D., Laverty, D., Weiner, S., and Horton, W.E., Jr. Intrajoint comparisons of gene expression patterns in human osteoarthritis suggest a change in chondrocyte phenotype. *J Orthop Res* **23**, 1128, 2005.
- Blanco, F.J., Guitian, R., Vazquez-Martul, E., de Toro, F.J., and Galdo, F. Osteoarthritis chondrocytes die by apoptosis. A possible pathway for osteoarthritis pathology. *Arthritis Rheum* **41**, 284, 1998.
- Zamli, Z., Adams, M.A., Tarlton, J.F., and Sharif, M. Increased chondrocyte apoptosis is associated with progression of osteoarthritis in spontaneous Guinea pig models of the disease. *Int J Mol Sci* **14**, 17729, 2013.
- Athanasiou, K.A., DuRaine, G.D., Darling, E.M., Hu, J.C., and Reddi, A.H. *Articular Cartilage*. Boca Raton, FL: CRC Press/Taylor & Francis, 2013.
- Tew, S.R., Kwan, A.P., Hann, A., Thomson, B.M., and Archer, C.W. The reactions of articular cartilage to experimental wounding: role of apoptosis. *Arthritis Rheum* **43**, 215, 2000.
- Redman, S.N., Douthwaite, G.P., Thomson, B.M., and Archer, C.W. The cellular responses of articular cartilage to sharp and blunt trauma. *Osteoarthritis Cartilage* **12**, 106, 2004.
- Katoh, Y., and Shozo, T. Isolation of highly purified chondrocytes. *J Tissue Cult Methods* **6**, 103, 1980.
- Khaghani, S.A., Denyer, M., Youseffi, M., Lobo, S.B., and Javid, F.A. Purification of primary chondrocyte cells extracted from knee joint of Sprague-Dawley rats. The Anatomical Society Winter Meeting. Oxford, UK, 2009.
- Liu, J., Zhao, B., Zhang, Y., Lin, Y., Hu, P., and Ye, C. PHBV and predifferentiated human adipose-derived stem cells for cartilage tissue engineering. *J Biomed Mater Res A* **94**, 603, 2010.
- Jang, Y., Koh, Y.G., Choi, Y.J., Kim, S.H., Yoon, D.S., Lee, M., and Lee, J.W. Characterization of adipose tissue-derived stromal vascular fraction for clinical application to cartilage regeneration. *In Vitro Cell Dev Biol Anim* **51**, 142, 2015.
- Crevensten, G., Walsh, A.J., Ananthkrishnan, D., Page, P., Wahba, G.M., Lotz, J.C., and Berven, S. Intervertebral disc cell therapy for regeneration: mesenchymal stem cell implantation in rat intervertebral discs. *Ann Biomed Eng* **32**, 430, 2004.
- Woessner, J.F., Jr. The determination of hydroxyproline in tissue and protein samples containing small proportions of this imino acid. *Arch Biochem Biophys* **93**, 440, 1961.
- Athanasiou, K.A., Agarwal, A., Muffoletto, A., Dzida, F.J., Constantinides, G., and Clem, M. Biomechanical properties of hip cartilage in experimental animal models. *Clin Orthop Relat Res* **254**, 1995.

28. Athanasiou, K.A., Eswaramoorthy, R., Hadidi, P., and Hu, J.C. Self-organization and the self-assembling process in tissue engineering. *Annu Rev Biomed Eng* **15**, 115, 2013.
29. Roosendaal, G., Vianen, M.E., van den Berg, H.M., Laferber, F.P., and Bijlsma, J.W. Cartilage damage as a result of hemarthrosis in a human in vitro model. *J Rheumatol* **24**, 1350, 1997.
30. McIlwain, D.R., Berger, T., and Mak, T.W. Caspase functions in cell death and disease. *Cold Spring Harb Perspect Biol* **5**, a008656, 2013.
31. Bohm, I. Disruption of the cytoskeleton after apoptosis induction with autoantibodies. *Autoimmunity* **36**, 183, 2003.
32. Wickman, G.R., Julian, L., Mardilovich, K., Schumacher, S., Munro, J., Rath, N., Zander, S.A., Mleczak, A., Sumpton, D., Morrice, N., Bienvenut, W.V., and Olson, M.F. Blebs produced by actin-myosin contraction during apoptosis release damage-associated molecular pattern proteins before secondary necrosis occurs. *Cell Death Differ* **20**, 1293, 2013.
33. Guilak, F., Erickson, G.R., and Ting-Beall, H.P. The effects of osmotic stress on the viscoelastic and physical properties of articular chondrocytes. *Biophys J* **82**, 720, 2002.
34. Yang, P.J., and Temenoff, J.S. Engineering orthopedic tissue interfaces. *Tissue Eng Part B Rev* **15**, 127, 2009.
35. Berta, A., Duska, Z., Toth, F., and Hangody, L. Clinical experiences with cartilage repair techniques: outcomes, indications, contraindications and rehabilitation. *Eklek Hastalik Cerrahisi* **26**, 84, 2015.
36. Dhimolea, E. Canakinumab. *MAbs* **2**, 3, 2010.
37. Bernstein, L.R. Mechanisms of therapeutic activity for gallium. *Pharmacol Rev* **50**, 665, 1998.
38. Athanasiou, K.A., Responde, D.J., Brown, W.E., and Hu, J.C. Harnessing biomechanics to develop cartilage regeneration strategies. *J Biomech Eng* **137**, 020901, 2015.
39. Bonner, K.F., Daner, W., and Yao, J.Q. 2-Year postoperative evaluation of a patient with a symptomatic full-thickness patellar cartilage defect repaired with particulated juvenile cartilage tissue. *J Knee Surg* **23**, 109, 2010.
40. Choi, W.H., Kim, H.R., Lee, S.J., Jeong, N., Park, S.R., Choi, B.H., and Min, B.H. Fetal cartilage-derived cells have stem cell properties and are a highly potent cell source for cartilage regeneration. *Cell Transpl* **25**, 449, 2015.
41. Cook, J.L., Hung, C.T., Kuroki, K., Stoker, A.M., Cook, C.R., Pfeiffer, F.M., Sherman, S.L., and Stannard, J.P. Animal models of cartilage repair. *Bone Joint Res* **3**, 89, 2014.

Address correspondence to:  
*Kyriacos A. Athanasiou, PhD, PE*  
*Department of Biomedical Engineering*  
*University of California*  
*1 Shields Avenue*  
*Davis, CA 95616*

*E-mail: athanasiou@ucdavis.edu*

*Received: May 9, 2016*

*Accepted: August 23, 2016*

*Online Publication Date: September 2, 2016*